Supporting Information

Stumpp et al. 10.1073/pnas.1209174109

SI Validation of Selective Ion Electrode Measurements via BCECF in the Extracellular Matrix

To validate the selective ion electrode measurements, which were used to determine pH within the extracellular matrix (ECM), we additionally performed fluorimetric, noninvasive pH measurements using the pH-sensitive dye 2′,7′-bis-(carboxyethyl)-5(6)-carboxyfluorescein-acetoxymethylester (BCECF-AM) (Fig. S1).

Fluorimetric experiments were conducted as follows: To measure pH within the primary body cavity in larvae, we made use of xenobiotic transport—a mechanism usually used as a cellular defense mechanisms against toxins in aquatic organisms (multixenobiotic transport). Cleaved BCECF was exported from the cytosol of cells lining the gastric tract and subsequently trapped in the ECM of the body cavity. BCECF-AM (Invitrogen) stock solution of 10 mM in dimethyl sulfoxide (DMSO) (Invitrogen) was, in a first step, diluted with filtered seawater to 100 μM (1:100). Larvae (8–24 d postfertilization) were loaded with BCECF-AM in a second dilution step by mixing larval culture seawater including five to six individuals with BCECF/seawater solution. The final working solution had a BCECF concentration of 30 μM and a DMSO concentration of 0.3% (vol/vol). Animals were incubated in 30 μM BCECF-AM for 2 h at 12 °C in the dark. After incubation, larvae were washed five times with seawater and were kept at 12 °C in the dark for 60 min until fluorescence intensity in the primary body cavity was sufficient for detection. The procedure did not harm the animals: remaining individuals that were not used for the pH measurements survived a minimum of 7 d following the treatment. Late larvae (24 d postfertilization) close to settlement went through metamorphosis in the incubation tubes after the treatment with BCECF-AM.

pH_e measurements were conducted using an inverted confocal laser-scanning microscope (Leica; SP5) equipped with a perfusion system (comparable with the one used for the microelectrode measurements). Larvae were mounted in the perfusion bath at control pCO_2 conditions (pH 8.1) and held in place with a glass holding pipette to which a slight vacuum was applied (Fig. S4). The bath (volume of 0.5 mL) was perfused at a rate of 3 mL min^{-1} with seawater adjusted to different pHs by injection of pure CO_2 (pH 8.1, 7.7, 7.3, and 6.9; temperature of 13 ± 0.2 °C). Each larva (n = 7) was left to adjust to pH 8.1 for 10 min before the first pH change was introduced. pH was changed in the order of 8.1, 7.7, 7.3, 6.9, and back to control pH 8.1. Each pH was applied for 10 min. One experiment lasted 60–65 min. The recording interval was once per minute for 5 min postsolution change, one recording at 7 min postsolution change, and one at 10 min postsolution change to minimize dye bleaching throughout the experiment. With selected confocal laser settings, no detectible dye bleaching occurred. Two larvae exposed to the same experimental protocol, but only supplied with seawater adjusted to pH 8.1, served as control for fluorescence intensity drift over the experimental period. This way, an increase or decrease in pH_e due to potential active regulation of the larvae in response to elevated pCO_2 could be reliably detected. Because of high variations in fluorescence intensity ratios (ratios between 2.5 and 3.5) among individual larvae, data were normalized to the starting fluorescence intensity ratio at pH 8.1 of the respective larva.

For calibration of BCECF fluorescence intensity ratios, it was assumed that the extracellular fluid in the primary body cavity is similar in composition to seawater. BCECF-dextran (10 mM in dimethyl sulfoxide; Invitrogen) was diluted in artificial seawater adjusted to different pH to a final concentration of 50 μM. This concentration of BCECF-dextran yielded the same fluorescence intensity range when using the same confocal settings as BCECF-loaded larvae. To maintain stable pH values in seawater, artificial seawater (400 mM NaCl, 9.6 mM KCl, 52.3 mM $MgCl_2$, 9.9 mM $CaCl_2$, 27.7 mM Na_2SO_4) was buffered with 20 mM Tris·HCl. Measurements were conducted at 12 °C. For better comparison with values obtained in larvae, normalization was conducted by dividing all ratio values by the ratio measured at pH 8.1. The normalized ratio increased linearly with increasing pH up to a pH of 7.7. Between pH 7.7 and 8.1, almost no increase in ratio could be observed. This indicated a limited BCECF sensitivity for pH measurements in seawater.

The results confirm the high proton permeability of the ECM. However, as shown in the main article, the optimum range (linear part of the sigmoidal curve) for BCECF pH measurements in seawater lies between 6.5 and 7.5. Thus, the ratio changes for the pH steps 8.1–7.7 and 6.9 back to 8.1 have signal-to-noise ratios that prevent accurate measurements (Fig. S1).

For intracellular pH measurements using BCECF-AM, we removed the epithelial cells according to the description provided in the main article to reduce background noise. Clearly visible primary mesenchyme cells that were sufficiently loaded with the dye were used for the recordings (Fig. S5).

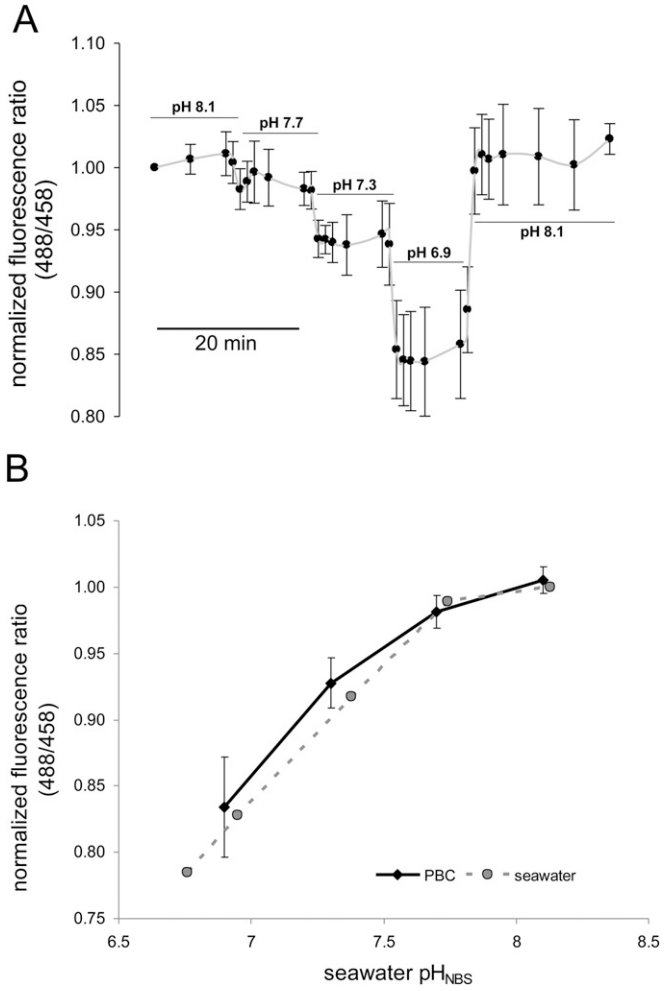

Fig. S1. Extracellular pH (pH_e) measurements in larvae of *Strongylocentrotus droebachiensis*. (*A*) BCECF fluorescence ratio is given as a measure of pH_e at different seawater (bath) pH values relative to starting ratio. pH_e follows seawater pH without significant compensation in the observation period. The effects are reversible without regulatory overshoot. (*B*) Correlation of fluorescence ratio from BCECF-dextran in seawater pH and BCECF-AM in PBC (n = 2 for BCECF-dextran in seawater; n = 7 for PBC measurements; mean ± SD). BCECF-dextran was normalized onto the ratio at pH 8.1. Note the decreasing slope of the calibration curve between pH 7.7 and pH 8.1 indicating the border of BCECF detection range in seawater similar to the slope decrease of the calibration curve of BCECF-AM in the primary mesenchyme cells (see *Results and Discussion* for details).

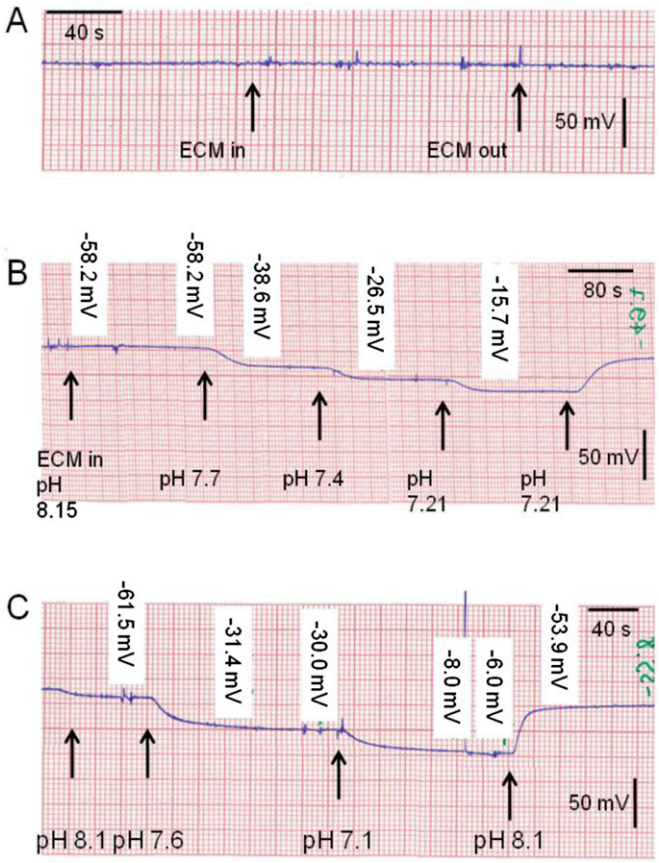

Fig. S2. Original recordings of voltage measurements (time line from *Left* to *Right*) using nonselective (*A*) or H^+-selective (*B* and *C*) microelectrodes. No potential difference was recorded during insertion of the electrode into as well as during removal from the ECM (*A*). pH steps recorded within the ECM demonstrating pH conformity to the environmental pH (*B*). pH steps recorded within the perfusion bath for electrode calibration (*C*). Note the slower response times within the ECM.

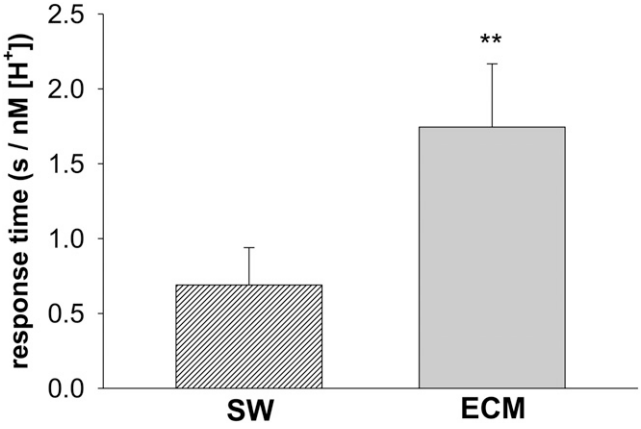

Fig. S3. Equilibration time of fluid exchange in the perfusion bath combined with the response time of the ion-selective electrode in seawater (SW) and within the extracellular matrix (ECM). Response time was calculated from the time needed to reach 95–100% of the fully stabilized value after a pH change between 8.1 and 7.2. For a linear relationship, differences in pH are expressed as H^+ concentrations. Bars represent ± SD; n = 10–12.

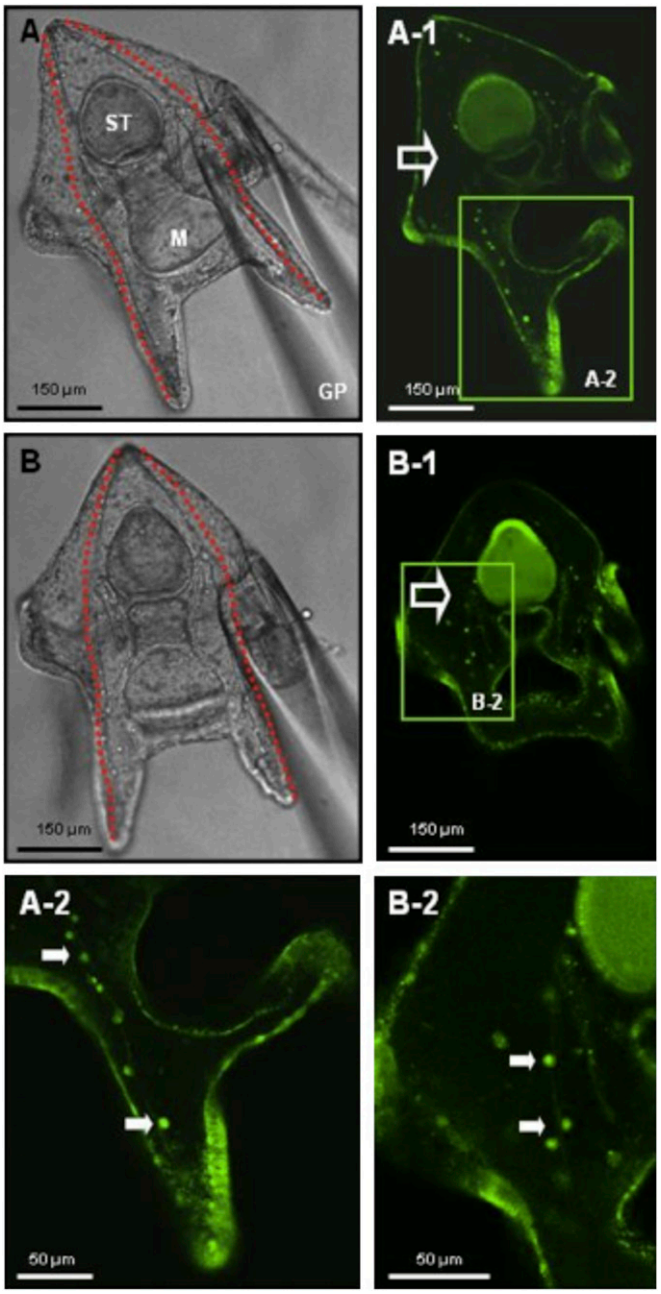

Fig. S4. In vivo confocal imaging of *S. droebachiensis* pluteus larvae (*A* and *B*). Primary mesenchyme cells along the calcitic spicules (PMCs, small arrows), the outer ectodermal epithelium, and digestive tract could be visualized in larvae loaded with BCECF-AM and exposed to probenecid. pH measurements in the extracellular environment directly surrounding the PMCs (large arrow) were performed with microelectrodes and microfluorimetrically (*SI Text*). The primary body cavity (large arrows) is filled with a collagen-glycoprotein matrix. GP, holding glass pipette; M, mouth; ST, stomach; spicules are traced in red.

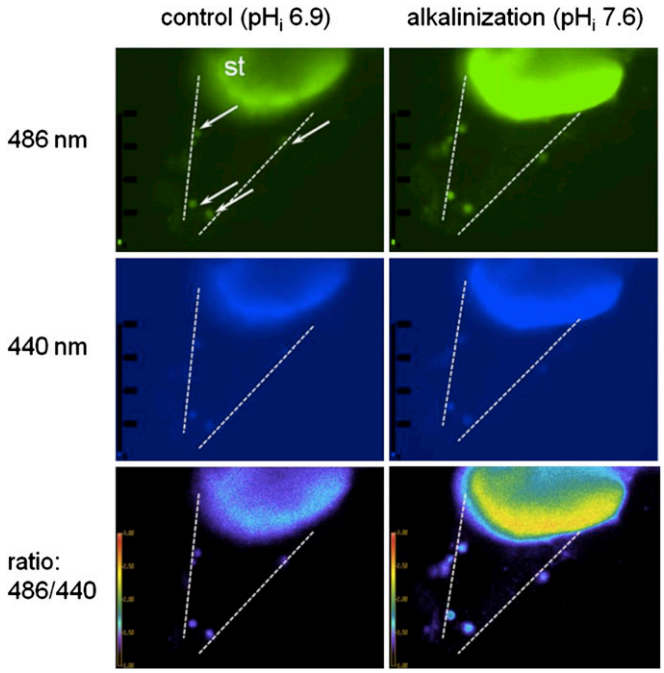

Fig. S5. Selected pseudo color images during BCECF recordings at 486-nm (first row) and 440-nm (second row) excitation and of the emission ratio (third row). A strong signal was emitted by the stomach (st) cells, which were clearly separated from the primary mesenchyme cells (indicated by arrows). During NH_3/NH_4^+-induced alkalosis, ratios increased steadily, corresponding to a rise in pH from pH$_i$ 6.9 until the plateau was reached at pH$_i$ 7.6. The dashed lines indicate the location of the two spicules.

Table S1. Intracellular pH values from microfluorimetry experiments

Baseline pH$_i$	Treatment after prepulse	Acidosis pH$_i$	Recovery pH$_i$	Recovery ΔpH$_i$	Recovery rate, ΔpH$_i$ min^{-1}	*n*
7.18 ± 0.20	ASW	6.50 ± 0.06	7.13 ± 0.20	0.64 ± 0.17	0.047 ± 0.011	5
6.82 ± 0.16*	5 mM Na^+	6.32 ± 0.10**	6.44 ± 0.06**	0.13 ± 0.05**	0.015 ± 0.009**	5
6.64 ± 0.22	ASW	6.34 ± 0.16	6.58 ± 0.17	0.25 ± 0.07	0.041 ± 0.009	4
6.71 ± 0.22	0 mM HCO_3^-	6.40 ± 0.15	6.42 ± 0.15	0.02 ± 0.01**	0.008 ± 0.007**	4
6.77 ± 0.19	ASW	6.40 ± 0.21	6.71 ± 0.19	0.32 ± 0.04	0.042 ± 0.023	4
6.96 ± 0.28	amiloride	6.55 ± 0.34	6.72 ± 0.31	0.17 ± 0.11*	0.033 ± 0.015	5

Comparison of pH$_i$ values, changes (ΔpH), and recovery rates (ΔpH$_i$ min^{-1}), after NH_4Cl withdrawal from experiments as shown in Fig. 5. *$P < 0.05$; **$P < 0.01$.

Table S2. Seawater physicochemical conditions

Incubation group	Temperature, °C	Salinity	pH	Ω_{Ca}	Ω_{Ar}	CO_2, ppm	Cτ
Control	9.42 ± 0.95	31.7 ± 0.14	8.06 ± 0.02	3.84 ± 0.30	2.42 ± 0.19	449.7 ± 45.4	2,582.1 ± 13.4
CO_2, ~1,120 ppm	9.43 ± 0.96	31.7 ± 0.09	7.73 ± 0.03	1.94 ± 0.04	1.22 ± 0.02	1,015.1 ± 12.4	2,695.9 ± 42.4
CO_2, ~2,400 ppm	9.48 ± 0.94	31.8 ± 0.08	7.39 ± 0.02	0.88 ± 0.01	0.55 ± 0.01	2,457.8 ± 17.0	2,839.4 ± 23.7

Seawater physicochemical conditions during hypercapnia experiments (10 d each). C_T, total dissolved inorganic carbon; Ω_{Ca}, calcite saturation state; Ω_{Ar}, aragonite saturation state; pCO_2, partial pressure of CO_2;. Values are presented as mean ± SD.

Table S3. Artificial seawater solutions

	ASW	20 mM NH_3/NH_4^+	5 mM Na^+	0 BIC	ASW_{Nig}
Na^+	420	430	5	474	370
K^+	9.9	9.9	9.9	9.9	150
Mg^{2+}	53.3	48.3	53.3	53.3	53.3
Ca^{2+}	15.3	9.9	10.3	9.9	10
Cl^-	468.6	490	488.6	519.3	555.3
SO_4^{2-}	28.2	28.2	28	28	28
HCO_3^-	2.35	2.35	2.35	0	0
NH_4^+		20			
$NMDG^+$			443		
Hepes				5	
pH	8.2	8.2	8.2	8.2	
Osmolality	970 ± 10	971 ± 10	972 ± 10	973 ± 10	974 ± 10

Artificial seawater (ASW) solutions (concentrations given in $mmol \cdot kg^{-1}$).